Materials Research Proceedings 41 (2024) 1058-1067 https://doi.org/10.21741/9781644903131-116

Investigation on diametral compression of an aluminium alloy AA5005 using EBSD and microhardness measurements

FRANCILLETTE Henri[1,a *] and GARAND Christian[2,b]

[1]Univ Rennes, INSA Rennes, CNRS, ISCR UMR 6226, 35000 Rennes, France

[2]Univ Rennes, INSA Rennes, LGCGM, 35000 Rennes, France

[a]henri.francillette@insa-rennes.fr, [b]christian.garand@insa-rennes.fr

Keywords: Aluminium, Diametral, Compression, Microhardness, EBSD

Abstract. The study of the link between the mechanical behaviour of metallic materials and the inspection of their microstructure is a particularly important subject of investigation. The plastic deformation of a commercial aluminium alloy AA5005 is analyzed in this work using mainly diametral compression tests and different experimental techniques of observation and characterization. Uniaxial compression tests and microhardness measurements have also been carried out in the study. For the characterization of the specimens, Electron Back Scattering Diffraction (EBSD) has been used in order to ascertain the state of the microstructure of the material at different stages. Characterizations are performed with EBSD notably for the received state and after diametral compression followed by heat treatments at 400 °C.

Introduction

In the transportation industry, the use of lightweight metals with high specific mechanical resistances is an important part of research. In this context, aluminum alloys and particularly the 5xxx Al-Mg series are of great interest [1-4]. The study of the mechanical behaviour of aluminium alloys in relation to their microstructure is necessary to understand the practical use of this type of metals [5,6]. Among the possible mechanical tests, diametral compression, the usual uniaxial compression and Vickers microhardness measurements are used in the study to characterize a commercial AA5005 aluminium bar. The diametral compression test is a less common mechanical test. Historically, this latter test has been developed few decades ago in order to determine the mechanical strength of concrete cylinders and pharmaceutical tablets [7,8]. It allows the measurement of the strength of a material in an indirect way when tensile tests are difficult because of the properties of the material [7]. It has been used more recently for metallic glass [9] and for sprayed coated and uncoated circular disc specimens [10]. Diametral compression has been used also in the characterization of the mechanical behaviour of metals notably for tubes and rings [11-13]. Interesting applications of this test (compared to the uniaxial one) can be found particularly for nuclear materials when determination of ductility in circumferential directions is investigated [12]. One can notice the recent use of this test (ring compression test) to study the influence of heterogeneities in an aluminium 6006 [13]. In the study presented here, the advantage of diametral compression test compared to uniaxial compression is that when diametral compression is considered one can expect more heterogeneities in the deformed cross-sections of the specimens. For instance, the geometry of the deformed specimens is expected to be less isotropic in the compression plane for diametral compression. When we use microhardness and EBSD measurements, the characterization of ductility of the metallic material can give important informations to find the links between the microstructure and the mechanical behaviour. Furthermore, diametral compression has the advantage or interest to provide experimental results (obtained with compressive stress and strain components) complementary to the usual

compression test. In the next sections, after the presentation of the experimental procedure, we will present the experimental results with their analysis, followed by conclusion.

Experimental procedure

A commercial bar of an AA5005 aluminium alloy is investigated by the consideration of two positions of cylindrical specimens which are determined by the compression direction of the mechanical device. These positions correspond to diametral compression and correspond to the usual uniaxial compression. The diametral compression test represents however the main part of the study. Vickers microhardness measurements are also performed in order to characterize the microstructures after the compression tests and heat treatments at 400 °C. Microhardness measurements have already been mentioned for AA5005 alloy [14]. Generally, heat treatments of aluminium alloys notably in 2xxx and 7xxx series may introduce important strain hardening effects when plastic deformation is applied, due to precipitates. Relatively low stress levels are expected due to heat treatments in the alloy investigated in this study AA5005 [19]. The new insight of the study presented here concerning heat treatments of an aluminium alloy is mainly their application after plastic deformation by diametral compression. Without these treatments, practically, it is particularly difficult to determine texture evolution by EBSD after plastic deformation.

Cylindrical specimens with a diameter of 8 mm were cut from a received commercial cylindrical bar with the same diameter. In the study the initial height of the samples was fixed at 10 mm. The mechanical tests were performed with a 200 kN capacity Instron press. All the compression tests were carried out at room temperature with a 1 mm/min cross-head speed. The total time for each mechanical test was fixed at 300 s. Concerning the Vickers microhardness measurements, a Mitutoyo device was used with a load of 0.3 kg. For each hardness measurement, the mean value of the two diagonals of the indent was determined. Optical microscopy has been used for the observation of the microstructure and a Dino-Lite optical microscope for the determination of macrographs. Electron Back Scattering Diffraction (EBSD) was also used to ascertain the microstructures of the analyzed samples, notably the Oxford HKL EBSD system in a Jeol scanning electron microscope (SEM). This technique is efficient to relate the crystallographic orientation of the grains of the material to its mechanical properties [15-19]. For the preparation of the specimens, after mechanical polishing, a solution with 0.5 % hydrofluoric acid was considered. For the Vickers hardness measurements and the EBSD characterizations the specimens were systematically wrapped in a phenolic resin.

In the experimental part of the study, a comparison was first performed between specimens of the received material in the initial state and specimens recovered 1 h at 300 °C before the mechanical tests. This temperature of 300 °C was chosen sufficiently high to provide potentially stress level differences in the measurements. All the compression tests were performed at room temperature. Next, for specimens in the received state, a particular attention was paid to microhardness measurements for diametral compression and for heat treatments performed at 400°C during 0.5 h and 3 h. The EBSD technique was used in order to ascertain the evolution of the microstructure.

Results and analysis

The presentation of the microstructure of the received material in its initial state is given in Fig. 1 with sections corresponding to the inverse pole figures (IPF) of the horizontal X direction and the vertical Y direction, using the EBSD technique. The Y direction corresponds to the compression direction during diametral compression and the observation plane corresponds to a cross-section of the cylindrical bar before deformation. One can notice grains of the order of 100 μm or less. This cartography has been obtained with a step of the electron beam of 2 μm. The selected region corresponds to the center of the cylindrical surface. The crystallographic texture of the scanned zone of Fig.1 has been determined through the {100}, {110} and {111} pole figures plotted in

Fig. 2. We can notice a significant concentration of {100} poles along the normal of the observation plane.

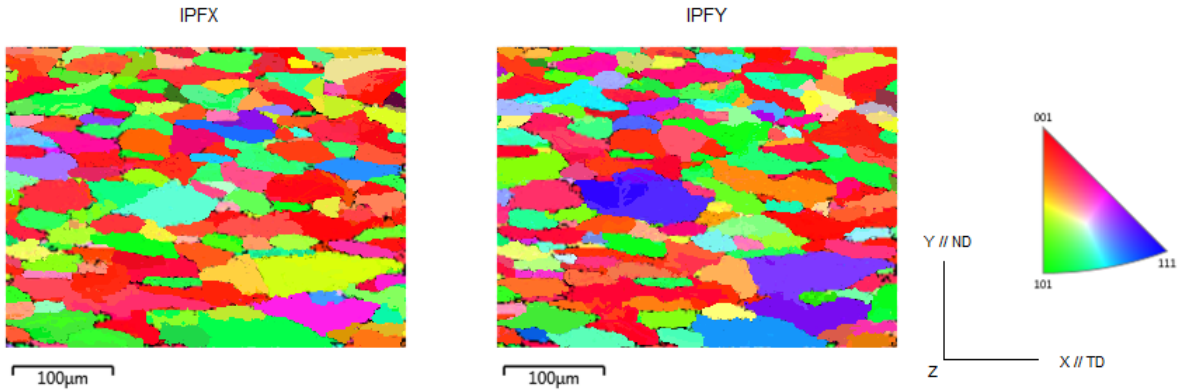

Fig. 1: EBSD characterization of the received material. The observation plane corresponds to a cross-section of the cylindrical specimens.

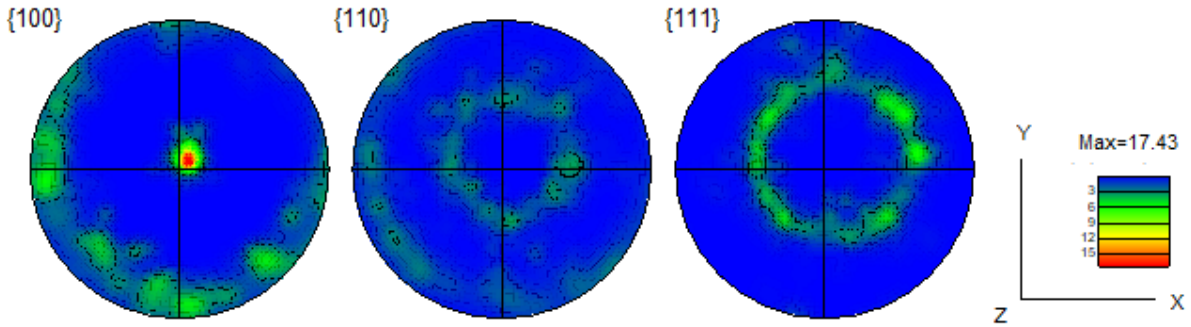

Fig. 2: Texture characterization of the received material : {100}, {110} and {111} pole figures. z along the axis of the initial cylinders.

The comparison of the mechanical tests for the received material and the material heat treated before the tests at 300 °C during 1 h are presented in the following figures. Fig. 3 and Fig. 4 correspond respectively to diametral compression and uniaxial compression at room temperature. For Fig. 3, the displacement u is normalized by the initial diameter d_0 of the specimen and the applied force F is normalized by the product of the initial diameter by the initial height h_0 of the specimen, as mentioned in the literature [9]. For uniaxial compression in Fig. 4, there is the presentation of the true stress-strain curves. We can notice greater values of the normalized force for the received specimen compared to the specimen recovered at 300 °C for a fixed value of the normalized displacement in Fig. 3. The same remark is true for the stress-strain curves of the uniaxial compression tests.

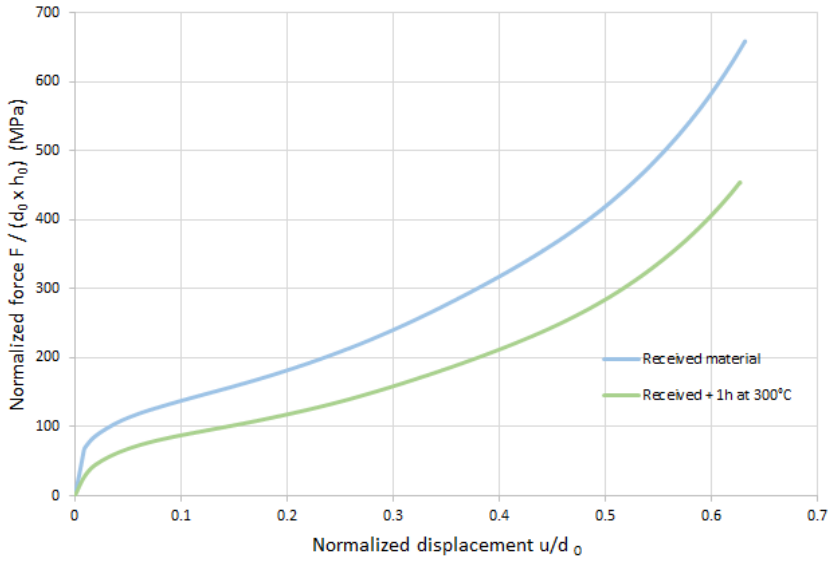

Fig. 3: Normalized force-displacement curves $F/(d_0 \times h_0)$ versus u/d_0 for diametral compression at room temperature for the received material and for the received material recovered 1 h at 300 °C before the test.

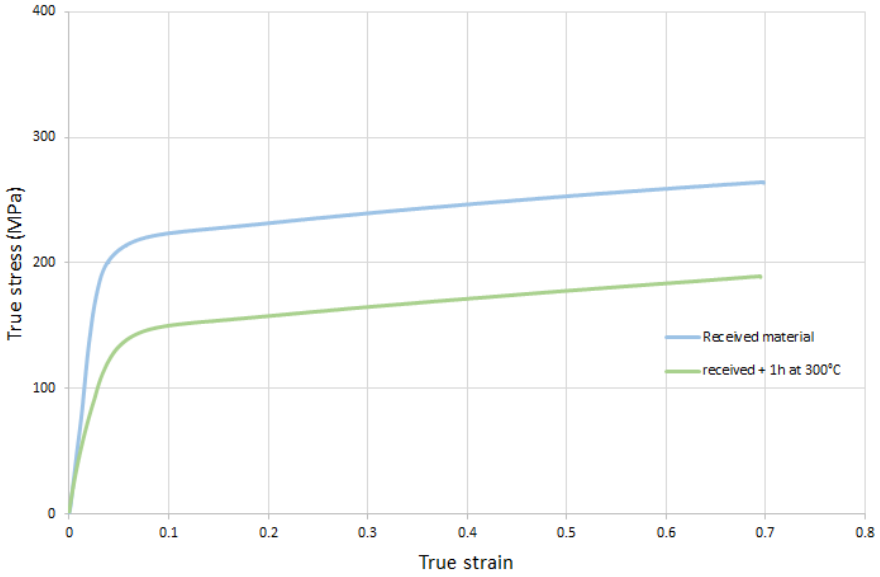

Fig. 4: True stress-strain curves of the uniaxial compression tests at room temperature for the received material and for the received material recovered 1 h at 300 °C before the test.

Macrographs of the compression surface of the specimens are presented in Fig. 5 after the mechanical tests. An irregular shape for diametral compression is obtained in Fig. 5(a) for which the compression direction corresponds to the normal of the figure and the initial axis of the (initial) cylinder (IAC) corresponds to the horizontal direction. Other macrographs of cross-sections are also presented in Fig. 6.

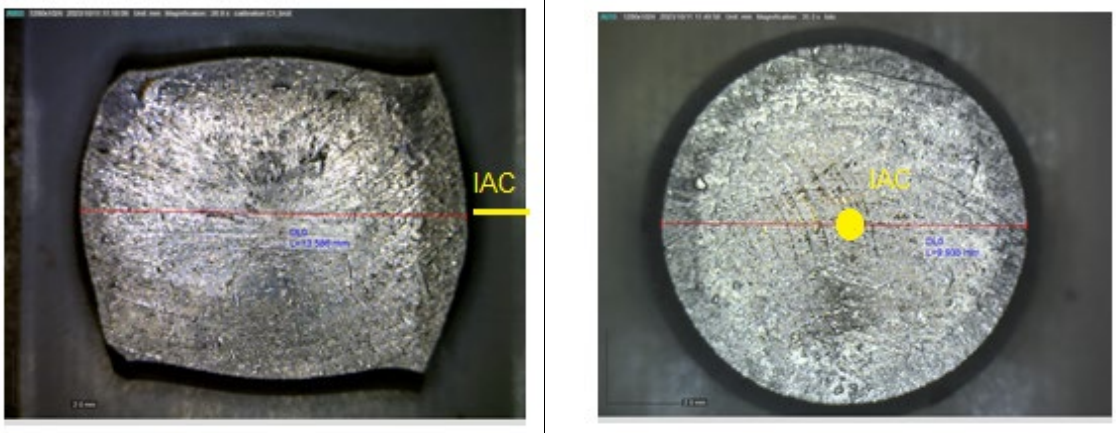

(a) (b)

Fig. 5: Macrographs of the compression plane of the specimens after the mechanical tests : (a) diametral compression (red line :13.586 mm) and (b) uniaxial compression (red line : 9.935 mm). The initial axis of the cylinder (IAC) is horizontal in (a) and along the normal of the figure in (b).

For Fig. 6(a) initially, before deformation, the section corresponds to a disc and Fig. 6(b) initially contains the initial axis of the cylindrical specimen. For the two sections, the compression direction (CD) is along the vertical direction of the figures.

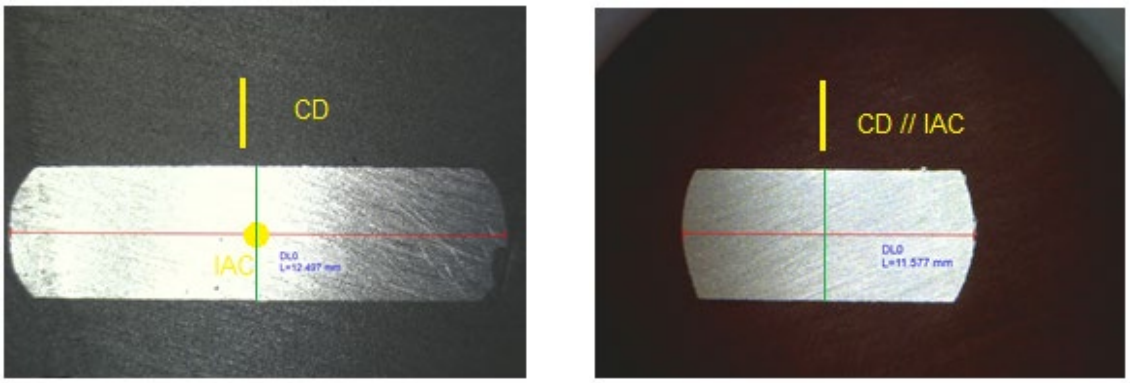

(a) (b)

Fig. 6: Macrographs of cross-sections after the mechanical tests: (a) diametral compression (red line : 12.497 mm) and (b) uniaxial compression (red line : 11.577 mm). The compression direction (CD) and the initial axis of the cylinder (IAC) are indicated in (a) and (b).

The evolution of Vickers hardness along two perpendicular lines (with extremities fixed as origins) of deformed specimens is considered experimentally for uniaxial compression and diametral compression, as illustrated in Fig. 6 by the colored lines. The comparison of the hardness values is performed for the uniaxial compression tests by considering firstly a specimen in the starting state of the received bar (without heat treatment) and secondly for a specimen with a recovery of 1 h at 300 °C before the mechanical test. The plane surface for which the measurements are performed corresponds to a section cutting the sample through its center and perpendicular to the observation plane of Fig. 5(b). The intersection between the plane of the measurements and the plane of observation of Fig. 5 (b) may be for example the visible red trace : it corresponds to Fig. 6(b). The lines for the Vickers microhardness measurements were selected in the following

Materials Research Proceedings 41 (2024) 1058-1067 https://doi.org/10.21741/9781644903131-116

way : line HC (Horizontal centered, or Central horizontal line) and line VC (Vertical centered, or Central vertical line). A step size of 200 µm and a load of 0.3 kg were taken into account for the microhardness measurements on the surfaces. Fig. 7 presents an illustration of experimental indents along two perpendicular lines (HC and VC) which have been performed during the measurements.

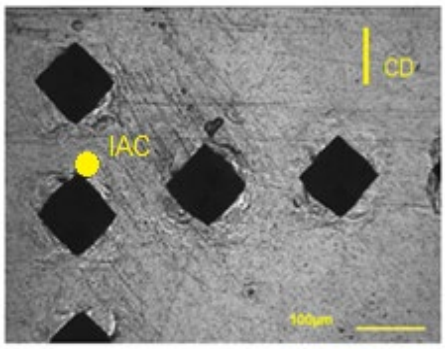

Fig. 7: Microhardness indents along horizontal and vertical centered lines (load of 0.3 kg) after diametral compression. The compression direction (CD) is vertical and the initial axis of the cylinder (IAC) is along the normal of the figure.

The experimental values are presented in Fig. 8 for uniaxial compression and in Fig. 9 for diametral compression. The origin of the axis for the distance corresponds in these figures respectively to the (left) beginning of the red lines and to the (top) beginning of the green lines illustrated in Fig. 6. The measurements indicate that the values are great along the horizontal line for the untreated sample with microhardness values close to 90.0 HV. Most of the values are near or greater than 60.0 HV in the other case. In diametral compression, the values of the microhardness are relatively low at the extremities of the HC line, notably for the sample recovered at 300 °C during 1 h before the mechanical test. Values below 58.0 HV are obtained. In the next sections, only specimens in the received state before diametral compression are considered.

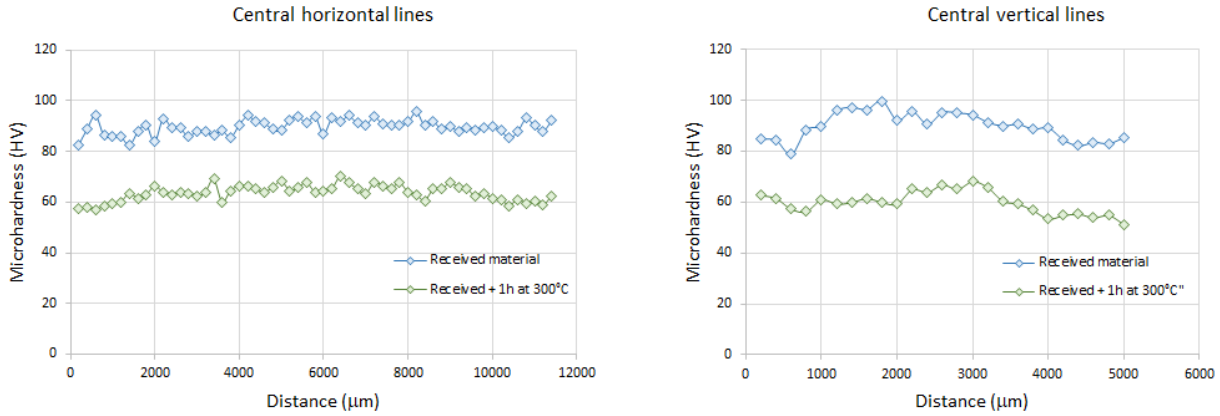

Fig. 8: Microhardness evolution in the specimens deformed by uniaxial compression at room temperature for the received material and for the material recovered 1 h at 300 °C before the test. Measurements (with origins) taken along the HC and VC lines (as illustrated in Fig. 6(b)).

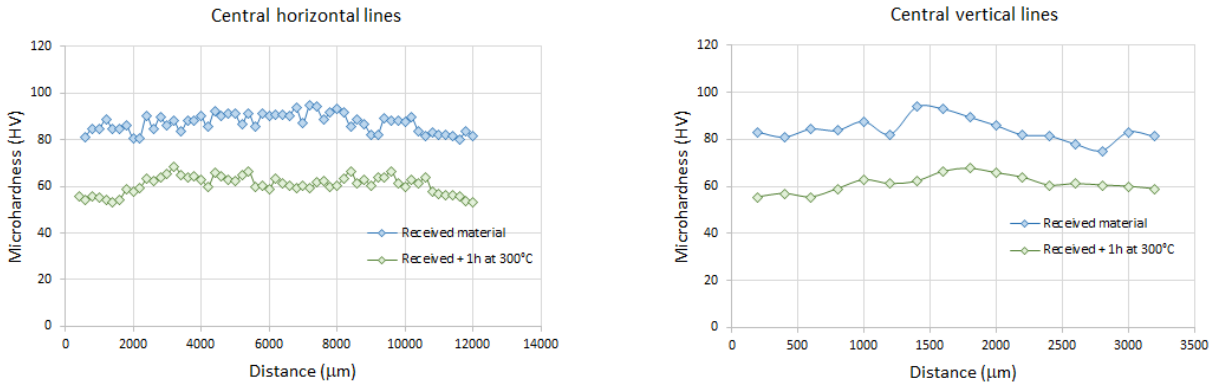

Fig. 9: Microhardness evolution in the specimens deformed by diametral compression at room temperature for the received material and for the material recovered 1 h at 300 °C before the test. Measurements (with origins) taken along the HC and VC lines (as illustrated in Fig. 6(a)).

In this section, the evolution of the microstructure is characterized after two heat treatments : in the first case, we consider 30 minutes at 400 °C and in the second case we consider 3 h at 400 °C. The corresponding microhardness measurements are presented in Fig. 10. We can observe lower values in the center of the central horizontal line for the curve corresponding to 30 minutes (values lower than 50.0 HV) compared to the extremities (values close to 55.0 HV - 60.0 HV). The values indicate a decrease of the hardness when the time of the heat treatment increases. On the one hand, Fig. 11 presents an ESBD analyzed zone at a short range for the specimen heat treated 0.5 h at 400 °C. A step size of 0.1 µm was chosen for the determination of this zone. The normal of the plane of observation is parallel to the initial axis of the initial cylinders and the compression direction (or normal direction ND) is in a vertical position. This also remains true for the next figure, notably Fig. 12. The microstructure in Fig. 11 is quite heterogeneous at this scale because of the previous plastic deformation of the specimen. For a greater heat treatment time at this temperature, notably 3 h at 400 °C, the microstructure is most regular at the grain scale. It was possible to determine a larger map for the orientation of the grains with EBSD. This corresponds to microstructure presented in Fig. 12. A step size of 2 µm was chosen for this map.

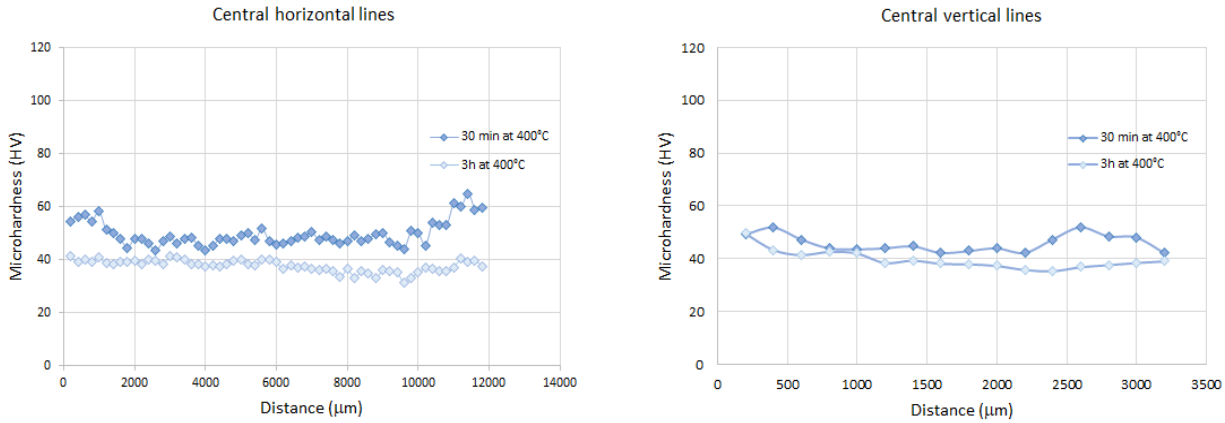

Fig. 10: Microhardness measurements of the received material deformed by diametral compression and recovered 0.5 h at 400 °C and 3 h at 400 °C. Measurements in a plane as in Fig. 6(a).

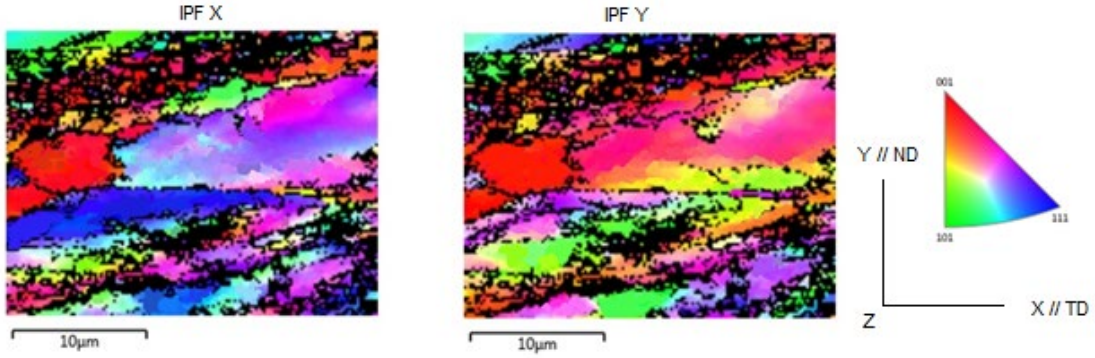

Fig. 11: EBSD analysis of the received material deformed by diametral compression and recovered 0.5 h at 400 °C : Inverse pole figures (IPF).

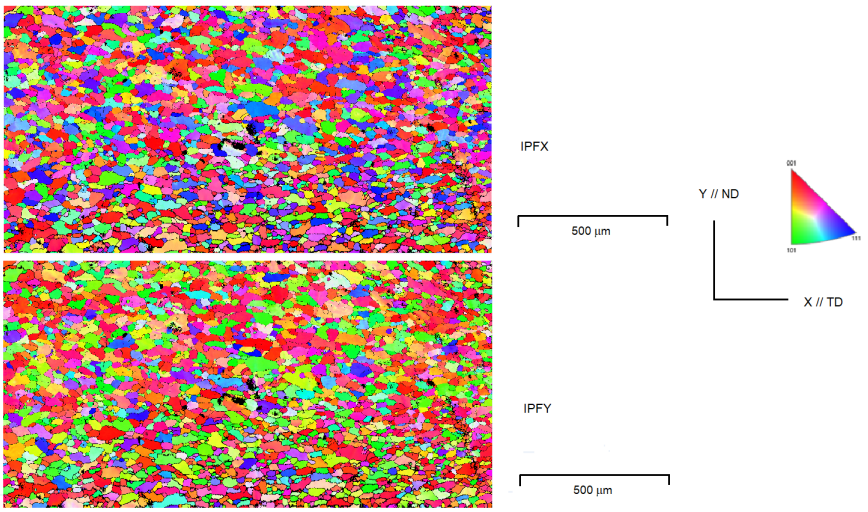

Fig. 12: EBSD zone analysis for the received material deformed by diametral compression and recovered 3 h at 400 °C.

To follow the crystallographic texture, the {100}, {110} and {111} pole figures associated with the analyzed zone of Fig. 12 were determined. The corresponding results are presented in Fig. 13. The vertical direction corresponds to normal direction (ND) during the mechanical test. We still observe an important concentration of {100} poles along the center of the pole figure. However, there is the appearance of poles in the vicinity of the compression direction.

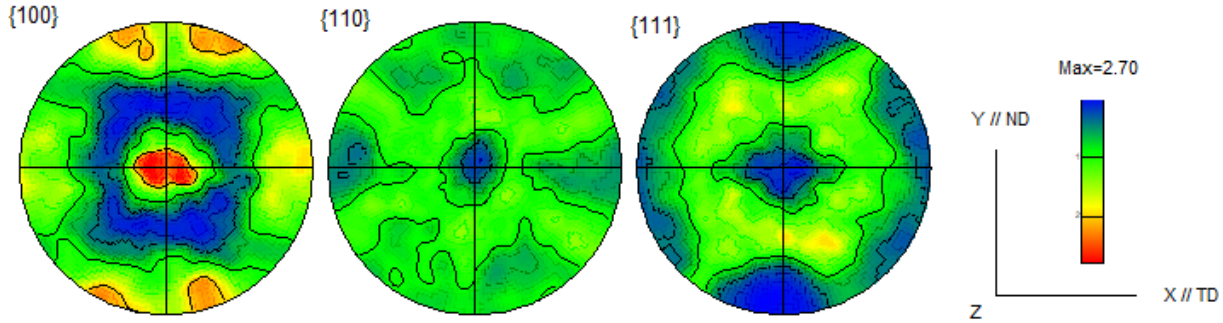

Fig. 13: Texture characterization of the received material deformed by diametral compression and recovered 3 h at 400 °C : {100}, {110} and {111} pole figures.

Conclusion

Specimens of an aluminium alloy AA5005 have been investigated in this study using different mechanical tests and different experimental techniques. Diametral compression tests were carried out and completed with uniaxial compression tests and Vickers microhardness measurements. Samples with a height of 10 mm and with a diameter of 8 mm were cut from a received rod, deformed and heat treated. The EBSD technique in a SEM has been used to ascertain the microstructures by the determination of the orientation of the grains and crystallographic textures. Different conditions have been considered for the compression tests at room temperature. Normalized force-displacement curves were plotted for the diametral compression tests and indicated significant level differences. The results are consistent with the corresponding uniaxial compression tests and the associated microhardness measurements. For the two heat treatments performed at 400 °C during 0.5 h and 3 h at 400 °C after plastic deformation, the microhardness measurements indicate a significant decrease compared to the state of the material after diametral compression. The new insights in the study concerning the influence of heat treatments on an aluminium alloy concern their effects on texture evolution after plastic deformation performed by diametral compression, and the corresponding characterization thanks to the use of the EBSD technique. The heat treatments were practically compulsory in this study for performing EBSD measurements because of strain hardening introduced before by diametral compression. The EBSD analysis indicates local heterogeneities in the microstructure at the grain scale after 0.5 h compared to 3 h. An important concentration of the {100} poles along the initial direction of the axis of the initial cylinders is still measured after the heat treatment of 3 h at 400 °C.

References

[1] A. Weck, P. Bisaillon, L. Nong, T. Meunier, H. Jin, M. Gallerneault, Mechanical properties of the aluminium roll-bond laminate AA5005- AA5083-AA5005. Mater. Sci. and Eng. A 528 (2011) 6186-6193. https://doi.org/10.1016/j.msea.2011.04.037

[2] J. Hirsch, T. Al-Samman, Superior light metals by texture engineering : Optimized aluminium and magnesium alloys for automotive applications. Acta Mater. 61 (2013) 818-843. https://doi.org/10.1016/j.actamat.2012.10.044

[3] H. Francillette, C. Garand, Formability and macroscopic shearing of a titanium alloy Ti-6Al-4V under channel die compression. AIP Conference Proceedings 1896, 020005 (2017). https://doi.org/10.1063/1.5007962

[4] D. Scotto D'Antuono, J. Gaies, W. Golumbfskie, M.L. Taheri, Direct measurement of the effect of cold rolling on β phase precipitation kinetics in 5xxx series aluminium alloys. Acta Mater. 123 (2017) 264-271. https://doi.org/10.1016/j.actamat.2016.10.060

[5] P.B. Trivedi, R.S. Yassar, D.P. Field, R. Alldredge, Microstructural evolution and observed stress response during hot deformation of 5005 and 6022 Al alloys. Mater. Sci. and Eng. A 425 (2006) 205-212. https://doi.org/10.1016/j.msea.2006.03.059

[6] F. Shen, D. Yi, B. Wang, H. Liu, Y. Jiang, C. Tang, B. Jiang, Semi-quantitative evaluation of texture components and anisotropy of the yield strength in 2524 T3 alloy sheets. Mater. Sci. and Eng. A 675 (2016) 386-395. http://dx.doi.org/10.1016/j.msea.2016.08.013

[7] V. Mazel, S. Guerard, B. Croquelois, J.B. Kopp, J. Girardot, H. Diarra, V. Busignies, Reevaluation of the diametral compression test for tablets using the flattened disc geometry. International journal of pharmaceutics 513 (2016) 669-677. http://dx.doi.org/10.1016/j.ijpharm.2016.09.088

[8] M. Mellor, I. Hawkes, Measurement of tensile strength by diametral compression of discs and annuli. Eng. Geol. 5 (3) (1971) 173-225. https://doi.org/10.1016/0013-7952(71)90001-9

[9] C. Bernard, S. Hin, L. Charleux, E. Roux, Y. Yokoyama, A. Tanguy, V. Keryvin, Intense shear band plasticity in metallic glass as revealed by a diametral compression test. Mater. Sci. and Eng. A 864 (2023) 144533. https://doi.org/10.1016/j.msea.2022.144533

[10] N.H. Faisal, L. Mann, C. Duncan, E. Dunbar, M. Clayton, M. Frost, J. McConnachie, A. Fardan, R. Ahmed, Diametral compression test method to analyse relative surface stresses in thermally sprayed coated and uncoated circular disc specimens. Surface and Coat. Tech. 357 (2019) 497-514. https://doi.org/10.1016/j.surfcoat.2018.10.053

[11] N. K. Gupta, G.S. Sekhon, P.K. Gupta, Study of lateral compression of round metallic tubes. Thin-walled structures 43 (2005) 895-922. https://doi.org/10.1016/j.tws.2004.12.002

[12] Y. Coget, Y. Demarty, C. Czarnota, A. Bracq, J.S. Brest, A. Rusinek, Lateral ring compression test applied to a small calibre steel jacket : Identification of a constitutive model. Defence technology. In Press. https://doi.org/10.1016/j.dt.2023.11.001

[13] L. Bizet, L. Charleux, P. Balland, L. Tabourot, Influence of heterogeneities introduces into the modelling of a ring compression test. Arch. of Civ. and Mech Eng. 17 (2017) 365-374. http://dx.doi.org/10.1016/j.acme.2016.11.002

[14] R. Abrahams, J. Mikhail, P. Fasihi, Effect of friction stir process parameters on the mechanical properties of 5005-H34 and 7075-T651 aluminium alloy. Mater. Sci. and Eng. A 751 (2019) 363-373. https://doi.org/10.1016/j.msea.2019.02.065

[15] I. Carneiro, S. Simöes, Recent advances in EBSD characterization of metals. Metals (2020) 10, 1097. https://doi.org/10.3390/met10081097

[16] H. Francillette, Effects of the interaction length between hollow shapes : Application to a HCP metal under mechanical loading. Procedia Manufacturing 47 (2020) 1203-1210. https://doi.org/10.1016/j.promfg.2020.04.351

[17] H. Francillette, B. Bacroix, M. Gaspérini, J.L. Béchade, Grain orientation effects in Zr702α polycristalline samples deformed in channel die compression at room temperature. Acta mater. 46 (1998), 4131-4142. https://doi.org/10.1016/S1359-6454(98)00121-9

[18] G. Zhao, M. Sun, J. Li, H. Li, L. Ma, Y. Li, Study on quasi-in-situ tensile microstructure evolution law of 5052-O aluminium alloy based on EBSD. Materials Today Communications 33 (2022) 104572. https://doi.org/10.1016/j.mtcomm.2022.104572

[19] J. Xie, Y. Liang, F. Yan, J. Zhou, P. Du, W. Liu. Effect of high-pressure heat treatment on the recrystallization and recrystallization texture of CC 5005 aluminium alloy. Journ. of Mater. Res. Tech. 26 (2023) 2017-2027. https://doi.org/10.1016/j.jmrt.2023.08.018